© 2020. Published by The Company of Biologists Ltd | Development (2020) 147, dev186882. doi:10.1242/dev.186882

RESEARCH ARTICLE

Cell-fate plasticity, adhesion and cell sorting complementarily establish a sharp midbrain-hindbrain boundary

Gokul Kesavan, Anja Machate, Stefan Hans and Michael Brand*

ABSTRACT

The formation and maintenance of sharp boundaries between groups of cells play a vital role during embryonic development as they serve to compartmentalize cells with similar fates. Some of these boundaries also act as organizers, with the ability to induce specific cell fates and morphogenesis in the surrounding cells. The midbrain-hindbrain boundary (MHB) is such an organizer: it acts as a lineage restriction boundary to prevent the intermingling of cells with different developmental fates. However, the mechanisms underlying the lineage restriction process remain unclear. Here, using novel fluorescent knock-in reporters, live imaging, Cre/lox-mediated lineage tracing, atomic force microscopy-based cell adhesion assays and mutant analysis, we analyze the process of lineage restriction at the MHB and provide mechanistic details. Specifically, we show that lineage restriction occurs by the end of gastrulation, and that the subsequent formation of sharp gene expression boundaries in the developing MHB occur through complementary mechanisms, i.e. cell-fate plasticity and cell sorting. Furthermore, we show that cell sorting at the MHB involves differential adhesion among midbrain and hindbrain cells that is mediated by N-cadherin and Eph-ephrin signaling.

KEY WORDS: Midbrain-hindbrain boundary (MHB), Zebrafish, Cell sorting, Cell adhesion, Ephrin signaling

INTRODUCTION

The concept of boundaries between gene expression domains is central and crucial to our current understanding of organ development because some of these boundaries also act as organizers or local signaling centers (Kiecker and Lumsden, 2005; Dahmann et al., 2011). Organizers are groups of cells that instruct other cells in their vicinity to acquire specific developmental fates and this fundamental process is essential for proper embryonic development (Arias and Steventon, 2018). The midbrain-hindbrain boundary (MHB), also known as the isthmic organizer (midbrain-hindbrain organizer), is an example of such an organizer that forms at the interface of the midbrain (mesencephalon, mes) and the hindbrain (cerebellum, metencephalon, met), and is vital for the formation and function of both the midbrain and the cerebellum (Rhinn et al., 2006; Gibbs et al., 2017). Cells at these signaling centers secrete various morphogens such as Wnt and fibroblast growth factors (FGFs), which provide 'positional information' and help establish proper tissue patterning and cell fate commitment (Gibbs et al., 2017).

Center for Regenerative Therapies TU Dresden (CRTD), Technische Universität Dresden, Fetscherstr. 105, 01307 Dresden, Germany.

*Author for correspondence (michael.brand@tu-dresden.de)

G.K., 0000-0002-2828-1460; M.B., 0000-0002-3917-0416

Handling Editor: François Guillemot
Received 27 November 2019; Accepted 30 April 2020

In vertebrates, the interface between the expression domains of two transcription factors, Otx and Gbx, constitutes the MHB; in zebrafish, the MHB develops from the initially overlapping expression domains of Otx2 and Gbx1 that subsequently sort out and form a sharp boundary (Raible and Brand, 2004; Rhinn et al., 2003). During this process, morphogens such as Wnt and Fgf, and transcription factors such as engrailed 1, engrailed 2, Pax2, Pax5 and Pax8, sequentially induce MHB formation, and their subsequent interplay is crucial for the maintenance of the MHB (Rhinn and Brand, 2001; Wurst and Bally-Cuif, 2001; Raible and Brand, 2004; Rhinn et al., 2006; Dworkin and Jane, 2013). The above-mentioned factors (Otx, Gbx, Wnt1, Fgf8, Pax and Eng) make up the core of the MHB signaling machinery and any functional disruption of these factors interferes with patterning at the MHB (Dworkin and Jane, 2013; Gibbs et al., 2017).

Several studies using various vertebrate models have addressed whether the MHB also acts as a lineage restriction boundary, apart from its role as an organizer, and most studies argue in favor of the MHB also being a lineage restriction boundary (Zervas et al., 2004; Sunmonu et al., 2011). We have previously demonstrated the existence of a lineage restriction boundary at the zebrafish MHB using a combination of high-resolution time-lapse imaging, single-cell labeling and transplantation experiments (Langenberg and Brand, 2005; Langenberg et al., 2006). Our observations imply a cell-cell communication mechanism that restricts the migration of cells across the presumptive MHB but still permits cell movement within the group of cells on either side of the boundary. Thus, although it is known that Otx2 and Gbx1 establish their expression domains on either side of the MHB, the mechanisms by which this Otx-Gbx interface acts as a lineage restriction boundary, and the cell biological processes that prevent the intermingling of cells destined to dissimilar developmental fates, remain poorly understood.

Therefore, we have addressed these issues using the developing zebrafish as a model. Specially, we visualized the establishment of the MHB in real time by generating various novel fluorescent reporter and Cre driver lines for *otx2b*, *wnt1*, *gbx1*, *gbx2* and *fgf8a* using CRISPR/Cas9-mediated knock-in strategies (Kesavan et al., 2017, 2018). Using a combination of time-lapse imaging and Cre/lox-mediated lineage tracing, we show that lineage restriction at the MHB occurs by the end of gastrulation. Next, we demonstrate that cells indeed sort at the MHB to establish a sharp boundary and that the underlying molecular mechanisms include differential adhesion between prospective midbrain and hindbrain progenitors, with N-cadherin involvement and signaling through the Eph-ephrin pathway.

RESULTS

Initially overlapping gene expression domains segregate over time

The gene expression boundary abutting the *otx2b-gbx1* expression domains demarcates the MHB primordium. In order to visualize these developmental events in real time, we generated CRISPR/

Development (2020) 147, dev186882. doi:10.1242/dev.186882

Cas9-based knock-in zebrafish lines. The coding sequences for the reporters were knocked-in upstream of the corresponding ATG and were, thus, under the control of the endogenous promoter/enhancer elements (Fig. 1A). Importantly, as shown previously, reporter expression faithfully reproduces endogenous gene expression patterns (Kesavan et al., 2017, 2018).

To address Otx-Gbx boundary formation in real time, we used time-lapse imaging of *otx2b:HRAS-mKate2*; *gbx1:Venus* double transgenic embryos wherein cell membranes of the midbrain cells and hindbrain cells themselves were labeled, respectively. However, this process could only be visualized from tail bud stage onwards (10 h post fertilization, hpf) because of the time required for the reporter (mKate2 or Venus) to become functional, despite being fast-folding proteins. Nonetheless, an overlap in the expression of *otx2b* (midbrain, mKate2) and *gbx1* (hindbrain, Venus) can be observed at the neural plate during the one- to two-somite stage (10.5-11 hpf), as evidenced by the presence of cells that are double positive for both mKate2 and Venus (Fig. 1B). Importantly, these cells could only be observed close to the prospective MHB and were not present in the deeper cell layers of the expression domains of either *otx2b* or *gbx1* (Fig. 1B). Subsequently, around the 10-14 somite stage (15-16 hpf), this intermingling of double-positive midbrain-hindbrain cells resolved into a sharper boundary (Fig. 1B,C; Movie 1). Overlapping expression domains were completely absent by around 30 hpf. Additionally, at this time point, the double-positive cells, along with gaps that represent *otx2b*-derived cells within hindbrain domain, were also not visible (Fig. 1B). Together, these observations imply a sequence of events during MHB formation wherein an initial overlap in the expression domains of Otx and Gbx resolves into a sharp, non-overlapping boundary over time. The process by which such initially overlapping gene expression domains segregate to form sharp boundaries can involve multiple mechanisms, such as loss of cell identity (cell-fate plasticity) or cell sorting (Batlle and Wilkinson, 2012). Hence, we next investigated whether these mechanisms play a role in MHB formation.

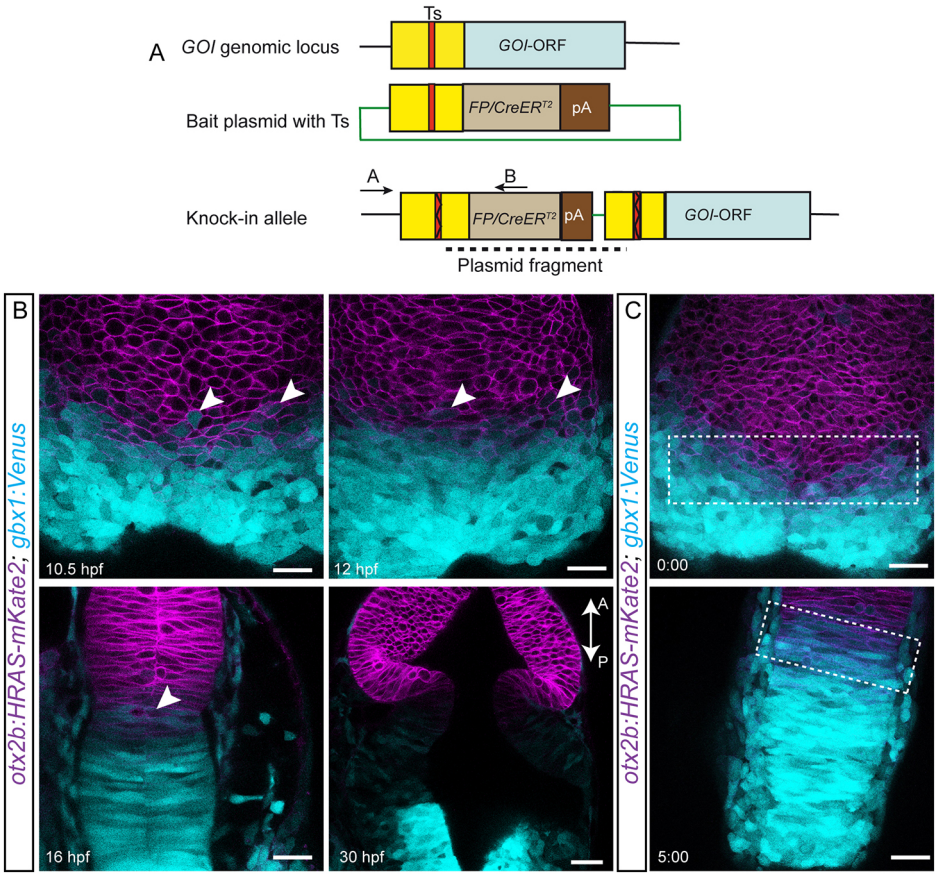

Fig. 1. Initially overlapping expression domains segregate over time. (A) The knock-in strategy used for generating transgenic fish is schematized. A target site (Ts) located upstream of the open reading frame (ORF) of a gene of interest (GOI) is chosen. A bait plasmid is constructed by cloning the sequence upstream of the ORF, including the target site. The bait plasmid, *sgRNA* against the target site and *Cas9* mRNA are injected into the embryo at the one-cell stage. The Cas9 protein creates double-stranded breaks at both Ts in the genomic locus and in the bait; this is followed by integration of the linearized bait plasmid. Only integration in the forward orientation will result in fluorescent reporter or *CreER^{T2}* expression. The primer pair (A+B) can be used to screen for and verify precise integration of the plasmid. The forward primer A is located outside the bait and the reverse primer B is located within the fluorescent reporter/*CreER^{T2}* sequence. (B) Live imaging was used to follow the expression of both mKate2 (membrane localized) and Venus, driven by the *otx2b* and *gbx1* locus, respectively, at the various time points indicated. Overlapping expression boundaries were initially observed during the segmentation stages, i.e. between 10.5 and 16 hpf, and these segregated over time, based on changes in the presence of double-positive cells (mKate2 and Venus positive, indicated with arrowheads). The above-described phenotype was consistently observed in multiple embryos, and the total number of embryos (*n*) analyzed for each stage are: 10.5 hpf (*n*=7), 12 hpf (*n*=7), 16 hpf (*n*=4) and 30 hpf (*n*=4). (C) Snapshots from the time lapse imaging movie are shown; the overlapping *otx2b-gbx1* region is indicated with a dotted rectangle. Time is shown in h:min. Scale bars: 20 µm. GOI, gene of interest; FP, fluorescent protein. The anterior-posterior axes of the embryos are marked with A-P and an arrow.

Development (2020) 147, dev186882. doi:10.1242/dev.186882

Lineage restriction at the MHB occurs at the end of gastrulation

To understand changes in cell identity, i.e. the establishment of lineage restriction at the midbrain-hindbrain boundary (MHB), we attempted two types of lineage tracing: short-term or transient labeling; and long-term or permanent tracing. We used both approaches in order to derive additional information on potential identity change or fate plasticity in the cells abutting the MHB. First, for short-term tracing, CRISPR/Cas9-mediated knock-ins of fluorescent reporters for multiple genes expressed at the MHB, i.e. *otx2b*, *wnt1*, *gbx1* and *gbx2*, were generated (Fig. 2A). Next, to follow the fate of Otx2- and Wnt1-expressing cells at the MHB, these fluorescent reporter lines were tagged with a nuclear localization signal (NLS) to generate *otx2b:Venus-NLS* and *wnt1:Venus-NLS* fish. Venus was used as the reporter because it is fast folding, which allows visualization of the early events during MHB formation. Moreover, it has a known lifetime of about 24 h (Li et al., 1998; Snapp, 2009), such that the 'perdurance' of the Venus protein,

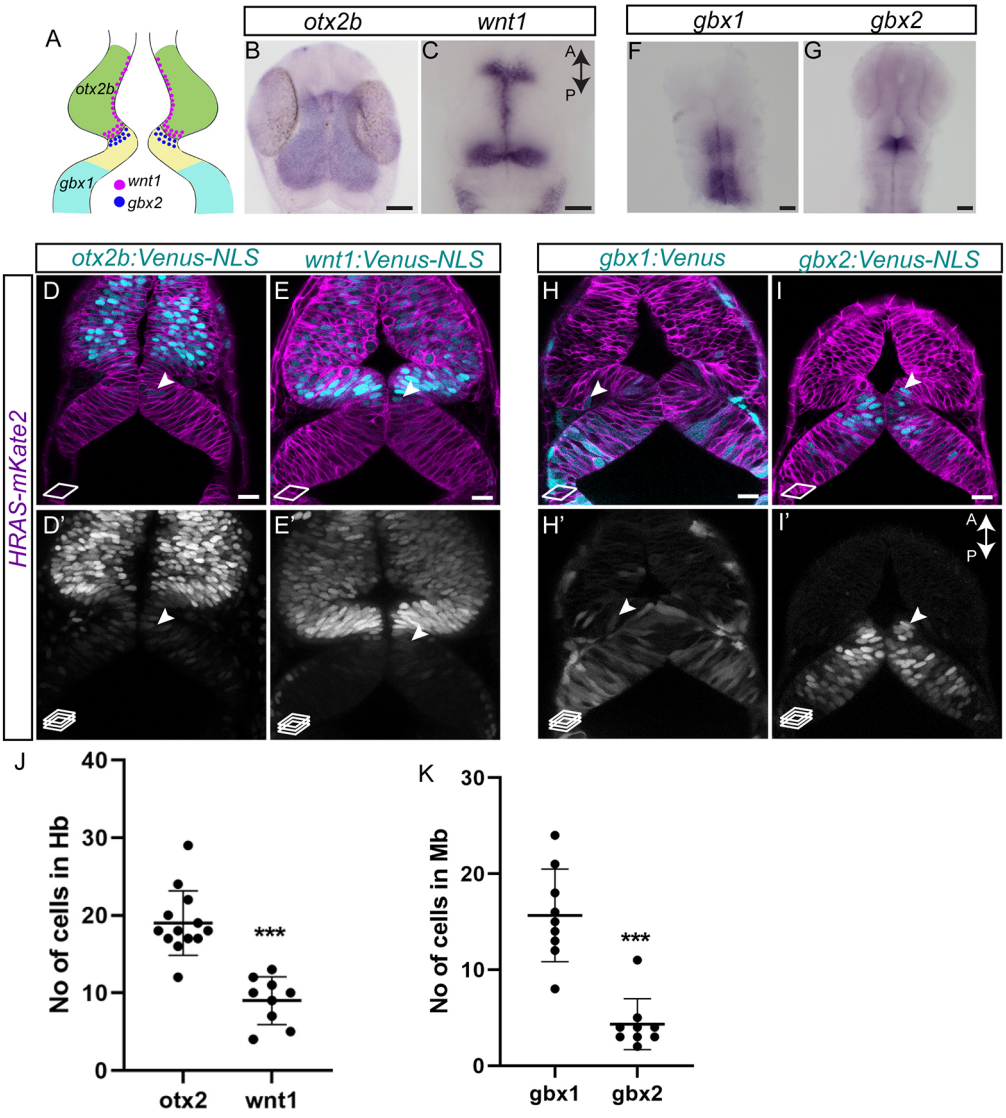

Fig. 2. Lineage restriction in the midbrain and the hindbrain occurs at the end of gastrulation. (A) Schematic representation of the various marker genes expressed at the MHB in a 24 hpf embryo. Midbrain-specific genes are *otx2b* (green) and *wnt1* (magenta dots); hindbrain-specific genes are *gbx1* (cyan) and *gbx2* (blue dots). (B,C) Whole-mount *in situ* hybridization (flat mount) for midbrain markers in 24 hpf embryos, i.e. *otx2b* and *wnt1*, show that their expression domains abut sharply at the MHB at this time point. (D,E,H,I) Venus fluorescent protein expression at 24 hpf in live embryos. Membrane-localizing mkate2 mRNA (red fluorescent protein) was injected into one-cell stage embryos to ubiquitously label all cells and visualize tissue architecture. (D,D′) *otx2b:Venus*-positive cells were not only present in the midbrain domain but also in the hindbrain domain (arrowheads). (E,E′) Similarly, *wnt1:Venus*-positive cells were present in the midbrain domain and were observed in the hindbrain domain (arrowheads). (F,G) Whole-mount *in situ* hybridization (flat mount) in 24 hpf embryos for hindbrain markers, i.e. *gbx1* and *gbx2*, shows discernible expression boundaries posterior to rhombomere 1 for *gbx1* and at the MHB for *gbx2* at this time point. (H,H′) In contrast to expression patterns seen in *in situ* hybridization, the *gbx1:Venus* transgenic line showed Venus-positive cells in the midbrain domain (arrowheads). (I,I′) In the *gbx2:Venus* transgenic line, very few Venus-positive cells could be observed in the midbrain domain, especially at the caudal midbrain domain (arrowheads). Images are from a single confocal plane in D,E,H,I, while the maximum projection images are shown in D′,E′,H′,I′. (J,K) Quantification of Venus-positive cells in their non-expression domains, i.e. *otx2b* and *wnt1* in the hindbrain, and *gbx1* and *gbx2* in the midbrain, shows that greater numbers of *otx2* and *gbx1* cells were present in their non-expression domains, compared with *wnt1* and *gbx2*, respectively. A two-tailed, unpaired *t*-test was used to calculate statistical significance. Each point in the graph represents an individual embryo with the mean and s.e.m. shown. *otx2* (n=13) versus *wnt1* (n=9), P<0.0001; *gbx1* (n=9) versus *gbx2* (n=9), ***P<0.0001. Scale bars: 10 µm in B,C,F,G; 20 µm in D,D′,E,E′,H,H′,I,I′.

Development (2020) 147, dev186882. doi:10.1242/dev.186882

even when the promoter is turned off, can be used as a lineage-tracing marker.

In situ hybridization at 24 hpf showed that *otx2b* and *wnt1* mRNA expression was restricted to the midbrain region with a sharp boundary abutting the MHB (Fig. 2B,C). In contrast, at 24 hpf, in the *otx2b:Venus* and the *wnt1:Venus* reporter embryos, the presence of Venus fluorescent protein (perdurance) was observed in the hindbrain domain, albeit with a weaker intensity than in the midbrain domain (Fig. 2D-E′), suggesting that these cells had indeed expressed *otx2b* and *wnt1* at an earlier time point during MHB development (Fig. S1). Furthermore, time-lapse imaging of *otx2b:Venus-NLS* and *wnt1:Venus-NLS* embryos not only showed the presence of Venus-positive cells in the hindbrain domain, but also that these cells remained within this domain over time (Movies 2 and 3). Taken together, these observations imply that cells abutting the MHB are indeed capable of changing their gene expression patterns and that they may display cell-fate plasticity.

Next, to verify whether a similar mechanism also operates in hindbrain cells, hindbrain boundary markers like *gbx1* and *gbx2* were lineage traced using *gbx1:Venus* and *gbx2:Venus-NLS* reporter lines. *In situ* hybridization at 24 hpf for hindbrain markers, i.e. *gbx1* and *gbx2*, showed expression boundaries posterior to rhombomere 1 for *gbx1* and at the MHB for *gbx2* (Fig. 2F,G). In contrast, at 24 hpf in the reporter fish, the presence of Venus fluorescent protein was observed in the midbrain domain, albeit with relatively weaker fluorescence intensity than that seen in the hindbrain domain (Fig. 2H-I′). Furthermore, as shown in Movie 1, these *gbx1*:*Venus*-positive cells were also *otx2b* positive and remained in the midbrain domain. Thus, these observations point to a pattern of perdurance of hindbrain markers (*gbx1*) in the midbrain domain and of midbrain markers (*otx2b* and *wnt1*) in the hindbrain domain.

Next, we quantified this perdurance and show that, on average, 19 *otx2b*:Venus-NLS-derived cells and 9 *wnt1*-derived cells per embryo were found in the hindbrain domain (Fig. 2J), i.e. greater numbers of *otx2b*-derived cells showed perdurance than did *wnt1*-derived cells. Similarly, although there were 15 *gbx-1*-derived cells in the midbrain, there were only four *gbx2*-derived cells (Fig. 2K). To understand why there may be more *otx2b* than *wnt1* cells, or more *gbx1* than *gbx2* cells, we evaluated gene expression onset by whole-mount *in situ* hybridization. The results revealed that *otx2b* expression occurs earlier than that of *wnt1* (6 hpf versus 10 hpf); likewise, *gbx1* expression occurs earlier (early onset) than that of *gbx2* (6 hpf versus 10 hpf) (Fig. S2), indicating that genes with earlier onset of expression may show greater plasticity compared with those showing later onset. Furthermore, these observations, when combined with the pattern of perdurance seen above, imply that lineage restriction occurs at the end of gastrulation in both midbrain and hindbrain cells.

Next, to substantiate that lineage restriction occurs at the end of gastrulation, we permanently labeled cells in the MHB region by generating CRISPR/Cas9-based CreER^{T2} knock-in lines and crossing them with a zebrabow responder line (Pan et al., 2013). Zebrabow-based lineage tracing allows stochastic recombination, and the resultant fluorescent protein combinations provide an opportunity to understand lineage decisions and clonal origins with high temporal resolution. CreER^{T2}-mediated recombination was induced with 4-hydroxy tamoxifen, administered at 6 hpf and/or 24 hpf, and all embryos were imaged at 48 hpf (Fig. 3A, schematic representation). In the *otx2b:CreER^{T2}* line combined with the zebrabow line, several recombined cells were observed in the hindbrain domain when 4-hydroxy tamoxifen was used at 6 hpf. In contrast, no recombined cells were seen upon 4-hydroxy tamoxifen induction at 24 hpf (Fig. 3B-C″). Similarly, the *fgf8a:CreER^{T2}* crossed with the zebrabow line revealed the presence of fgf8a-derived cells in the midbrain with 4-hydroxy tamoxifen induction at 6 hpf (Fig. 3D-D″). 4-Hydroxy tamoxifen induction at 24 hpf in this line did not yield a visible readout, probably because of low recombination efficiency and low Fgf8 expression (data not shown). These permanent lineage tracing results not only concur with the perdurance data described above, but also suggest that (1) lineage restriction indeed occurs at the end of gastrulation; and (2) there must be other mechanisms, such as cell sorting, that serve to subsequently establish and maintain sharp expression boundaries, i.e. from the tail bud stage onwards.

Cell sorting at the MHB

We looked at cell sorting as a possible mechanism of MHB formation and maintenance after lineage restriction was established at the tail bud stage. To track boundary cells with greater sensitivity in real time, we live imaged *wnt1:Venus-NLS* fluorescent reporter fish from the 1- to 2-somite stage until the 6- to 7-somite stage (10.5-12 hpf). We used Wnt1 as the marker because it accurately identifies midbrain boundary cells and, as mentioned earlier, imaging before 10 hpf was not possible due to the time required for reporter maturation. Using *z*-stacks of confocal images acquired over a narrow time interval (every 150 s), we were able to track individual cells (using labeled nuclei) with high spatial and temporal resolution (schematic representation of the cells tracked by time-lapse live imaging, Fig. 4A). All cells migrated only anteriorly and individual cell tracking of the *wnt1* cells showed zig-zag movements and crossovers among these cells (Fig. 4B-F and Movie 5). Furthermore, from around 14 hpf, when the neural rod has formed, cell movement was restricted and only inter-kinetic nuclear migration is observed (Movie 3), rather than active whole-cell movement. Interestingly, we could identify individual cells that were initially distant from the group of *wnt1*:*Venus-NLS*-positive boundary cells migrating anteriorly (Fig. 4B-E, arrowheads). We tracked the movement of one such straggling *wnt1*:*Venus-NLS*-positive cell and found that this cell actively migrated towards the group of other boundary cells (Fig. 4B-E, Movie 4). Such active migration of straggling *wnt1* cells was observed in multiple embryos (in five out of eight movies imaged; an additional time-lapse movie depicting such behavior is shown in Movie 6). We have also quantified the proportion of *wnt-1*-positive cells at a distance that sorted back to the midbrain (MB) domain. Enumerating such cells from time lapse movies (n=5) showed that about 50% of cells sorted back to the MB domain (51.6±11.9, mean±s.e.m.) (Table 1). Thus, it appears that cell sorting during MHB formation involves active cell mixing and migration of cells both within and between brain compartments, both of which may contribute to establishing sharp gene expression boundaries during neural rod formation.

Differential adhesion as a mechanism of cell sorting at the MHB

Proposed mechanisms of cell sorting include the differential tension hypothesis, the differential adhesion hypothesis and the repulsion hypothesis (Batlle and Wilkinson, 2012); here, we investigated whether differences in adhesion contribute to cell sorting at the MHB. Specifically, we used atomic force microscope-based single cell force spectroscopy (AFM-SCFS) (Fig. 5A, schematic representation of SCFS; Krieg et al., 2008) to determine potential differences in cell-cell adhesion properties of prospective midbrain and hindbrain cells.

Development (2020) 147, dev186882. doi:10.1242/dev.186882

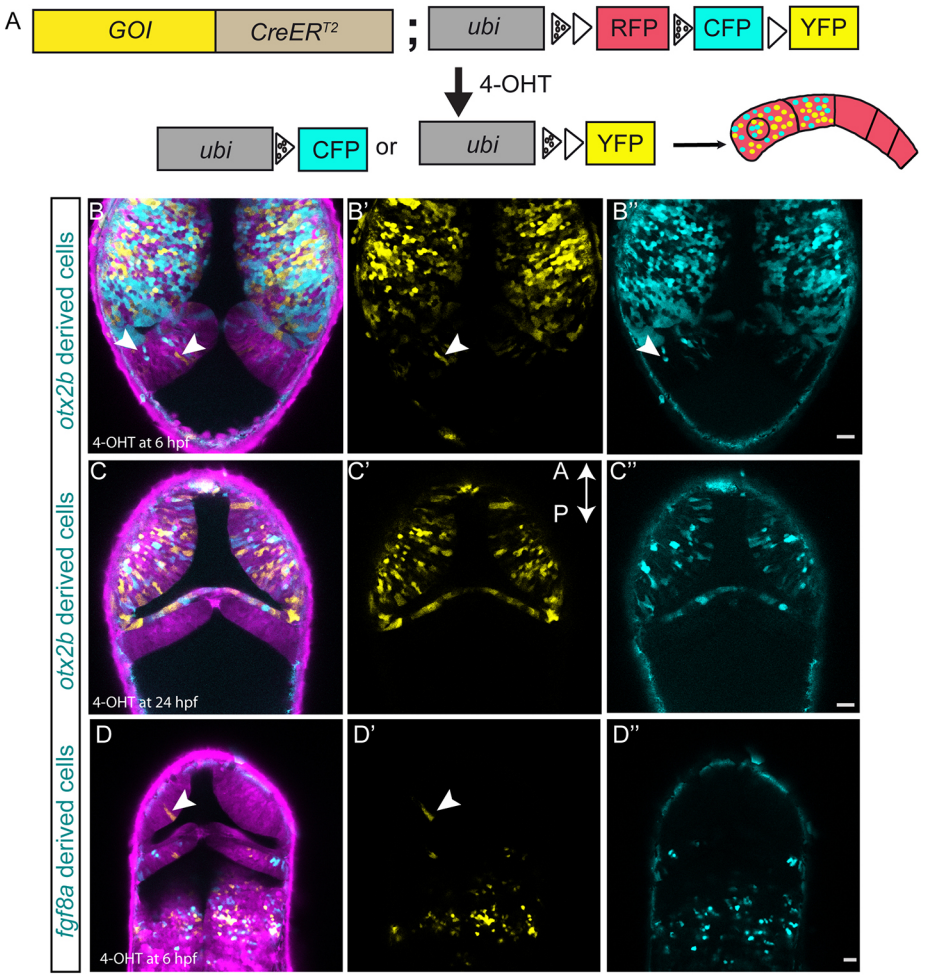

Fig. 3. Zebrabow-based lineage tracing to visualize lineage restriction patterns at the MHB. Multicolor-labeling of midbrain and hindbrain cells using the *otx2b:CreER*^{T2} and *fgf8a:CreER*^{T2} knock-in driver lines. (A) Schematic representation of *CreER*^{T2} -mediated recombination strategy using the zebrabow transgenic responder fish. In cells expressing CreER^{T2}, 4-OH-tamoxifen (4-OHT) induces recombination between either the two *lox2272* sites (marked by spotted triangles) or the two *loxp* sites (marked by a triangle), which results in the stochastic labeling of cells due to the expression of CFP (cyan fluorescent protein) or YFP in the recombined cells. All non-recombined cells express only RFP (red fluorescent protein). In a cell with multiple copies of RFP, CFP and YFP, CreER^{T2} -mediated stochastic recombination events lead to the formation of clones marked by different colors. Embryos obtained by crossing Cre driver fish (either *otx2b* or *fgf8a*) with the zebrabow responder line were treated with 4-OH-tamoxifen, either at 6 hpf (1 µM) or 24 hpf (10 µM) for 12 h; these embryos were live-imaged at 48 hpf. (B-B″) *otx2b:CreER*^{T2} embryos treated with 4-OHT at 6 hpf show effective recombination in the midbrain region but also a few recombined cells in the hindbrain region (arrowheads). (C-C″) *otx2b:CreER*^{T2} embryos treated with 4-OHT at 24 hpf show recombined cells only in the midbrain. (D-D″) Embryos of the *fgf8a:CreER*^{T2} knock-in driver line treated with 4-OHT at 6 hpf show effective recombination in the hindbrain with the exception of a few recombined cells in the midbrain (arrowheads). The above-described phenotype was consistently observed in multiple embryos, and the total number of embryos (*n*) analyzed for each condition are: *otx2b:CreER*^{T2} (4-OHT at 6 hpf, *n*=9; at 24 hpf, *n*=3); *fgf8a:CreER*^{T2} (4-OHT at 6 hpf, *n*=6). Scale bars: 20 µm.

Individual progenitor populations were isolated from various knock-in reporters such as the *otx2b:Venus* (for midbrain cells), *gbx1:Venus* (for hindbrain cells) and *dusp6:d2eGFP* transgenic line (for hindbrain cells) (Fig. 5B,C). Embryos were dissociated at the tail bud stage (10 hpf) and a single-cell suspension for AFM-SCFS was made by mechanical trituration (Fig. 5D,E). Measurements of the adhesive strength of progenitors of the same kind (homotypic adhesion or cohesion) showed that the midbrain cells have greater cohesion than hindbrain cells at both contact times tested (5 and 10 s; Fig. 5F). In contrast, adhesive forces between different cell types (heterotypic adhesion) were significantly lower than the cohesive force between two midbrain cells, but comparable with homotypic cohesion in hindbrain cells (Fig. 5G). These data imply the presence of differential adhesion between midbrain and hindbrain cells.

Calcium-dependent adhesion molecules (cadherins) are known to be essential for cell-cell adhesion during embryonic development. Therefore, to determine whether calcium is required for cohesion, we used EGTA to chelate calcium in the media and measured cohesion using AFM-SCFS. Calcium chelation dramatically reduced cohesive strength between midbrain cells and hindbrain cells, suggesting that cohesion is calcium dependent (Fig. 5H).

Next, as N-cadherin (N-cad, *cdh2*) is the major mediator of calcium-dependent adhesion, we used morpholinos to knockdown N-cad and demonstrate that the absence of N-cad led to a significant reduction in cohesive strength (Fig. 5I). Taken together, these findings suggest that the observed differential adhesion between midbrain and hindbrain cells requires calcium, and that it is primarily mediated by N-cad in the developing neural plate.

Molecular mechanisms of cell sorting at the MHB

To substantiate the above-described role of N-cad in cell-cell adhesion at the MHB, N-cadherin (*cdh2*) expression was perturbed

Development (2020) 147, dev186882. doi:10.1242/dev.186882

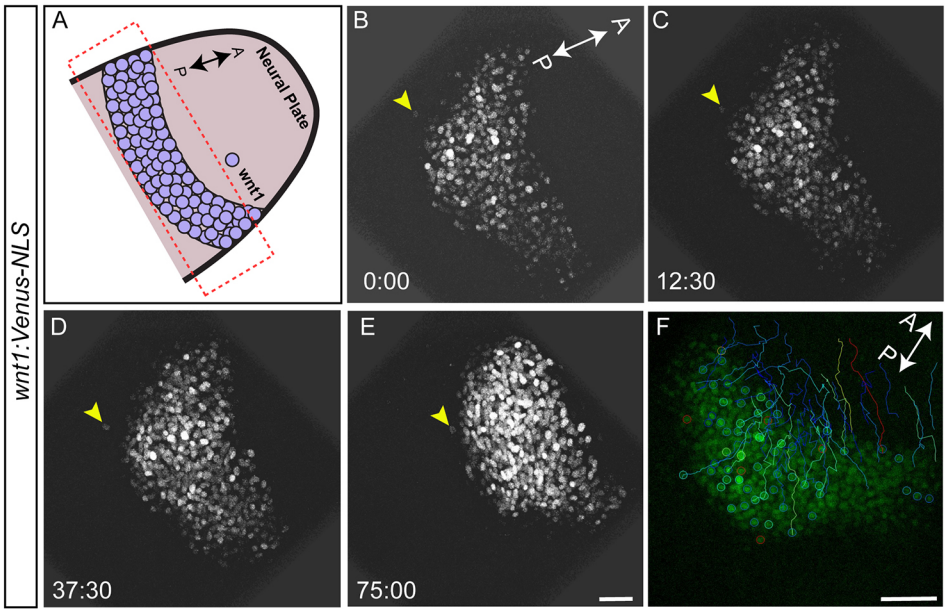

Fig. 4. Cells sort at the MHB. To visualize cell sorting during MHB development in real time, embryos from the *wnt1:Venus-NLS* reporter line were mounted and imaged dorsally between 10.5 and 12 hpf, such that the neural plate and the neural keel stages were captured. Tissue sections spanning about 30 µm were chosen with a *z*-interval of 1 µm. Images were acquired at 2:30 (min:s) intervals. (A) Schematic representation marking the area of interest (box) and the orientation of the embryo used for time-lapse imaging. (B-E) *wnt1:Venus-NLS*- positive cells in the midbrain are seen undergoing morphogenetic process such as neural plate convergence and migration towards the anterior end. Importantly, one *wnt1*:*Venus*-positive cell (arrowheads) that was separated from the rest of the boundary cells showed active migration towards the group of other boundary cells. Time is in min:s. (F) Cell tracking showing the intermingling of cells with zig-zag movements and crossovers of tracks. Of the eight embryos analyzed by time-lapse imaging, active cell sorting was observed in five (62.5%). Scale bars: 40 µm.

by two CRISPR/Cas9-mediated knockout approaches. In the first approach, global N-cad mutants were generated by injecting 2 sgRNAs targeting exon 1 and 2, along with Cas9 mRNA, in one-cell embryos. PCR genotyping showed efficient deletion and 'crispants' displayed phenotypes consistent with previously described *cdh2* mutants at 24 hpf (Jiang et al., 1996; Lele et al., 2002). Importantly, *in situ* hybridization showed disorganized gene expression boundaries for *otx2b* and *egr2b* in these mutants. In contrast, control fish showed clearly demarcated boundaries for these markers at 24 hpf. Additionally, in the N-cad mutants, individual *otx2b*-positive cells were visible outside their expression domain; again, such cells were absent in the control fish (Fig. 6A,B). In the second approach, N-cad was conditionally ablated in the otx2b domain using Cre/lox-controlled Cas9 combined with the *otx2b:CreER*^{T2} driver. This conditional perturbation of N-cad in the midbrain also resulted in irregular gene expression boundaries for *otx2b*, along with the presence of *otx2b*-positive cells outside the endogenous *otx2b* expression domain at 10 hpf (Fig. 6C,D). Thus, both targeted and global N-cad deficiency yielded very similar phenotypes. Taken together, these results imply that N-cad is necessary for establishing a sharp expression boundary for Otx2.

Table 1. Quantification of long-distance sorting based on nuclei tracking

Time-lapse movie number	Number of cells outside the MB domain	Number of cells that sorted back to MB domain (%)
Movie 1	5	4 (80%)
Movie 2	4	1 (25%)
Movie 3	8	3 (37.5%)
Movie 4	5	4 (80%)
Movie 5	3	1 (33.3%)

The Eph/ephrin signaling pathway is a known regulator of cell and tissue segregation during various stages of embryonic development (Xu et al., 1999). Importantly, it has been shown that the Eph receptor EphB4a is expressed in the midbrain (Cooke et al., 1997), while the ligand Efnb2a is expressed in a complementary manner in the hindbrain (rhombomere 1) (Cooke et al., 2005); we have observed the same expression pattern from late gastrulation stages (8-10 hpf). Therefore, to test whether Eph-ephrin signaling plays a role in cell sorting at the MHB, we expressed a truncated soluble form of Efnb2a (sol-efnb2a), which competes with various endogenous ephrin ligands that bind to Eph receptors, thereby disturbing both forward and reverse Eph/ephrin signaling (Cavodeassi et al., 2013; Cooke et al., 2001). Therefore, *sol-efnb2a* mRNA was injected into one-cell embryos of the *otx2b:HRAS-mKate2*, *gbx1:Venus* double transgenic line to monitor the Otx-Gbx gene expression boundary. Perturbed Eph-ephrin signaling resulted in mis-sorting of cells across the MHB and the presence of single *otx2b*-positive cells in the hindbrain. Additionally, *otx2b*-positive and *gbx1*-positive cells were seen distributed further from the Otx-Gbx overlapping domain compared with control embryos (Fig. 6E, Movies 7 and 8). These observations were confirmed by *in situ* hybridization for *otx2b* and *egr2b*, which revealed the presence of *otx2b*-positive cells outside their expression domain in the sol-efnb2a-injected embryos (Fig. 6F).

Finally, we used Cre/lox-based permanent labeling to understand the effects of disrupted Eph/ephrin signaling in lineage restriction and cell sorting at the MHB. Specifically, *fgf8a:CreER*^{T2} fish were crossed with the *Tg(hsp70l:loxP-DsRed-loxP-EGFPNLS)* to not only visualize sorting defects, but also enumerate the number of cells that have mis-sorted. Embryos exposed to 4-hydroxy-tamoxifen at 6 hpf and imaged at 36 hpf revealed the presence of *fgf8a*-derived cells in the midbrain. Notably, when s-efnb2a mRNA was injected in these

Development (2020) 147, dev186882. doi:10.1242/dev.186882

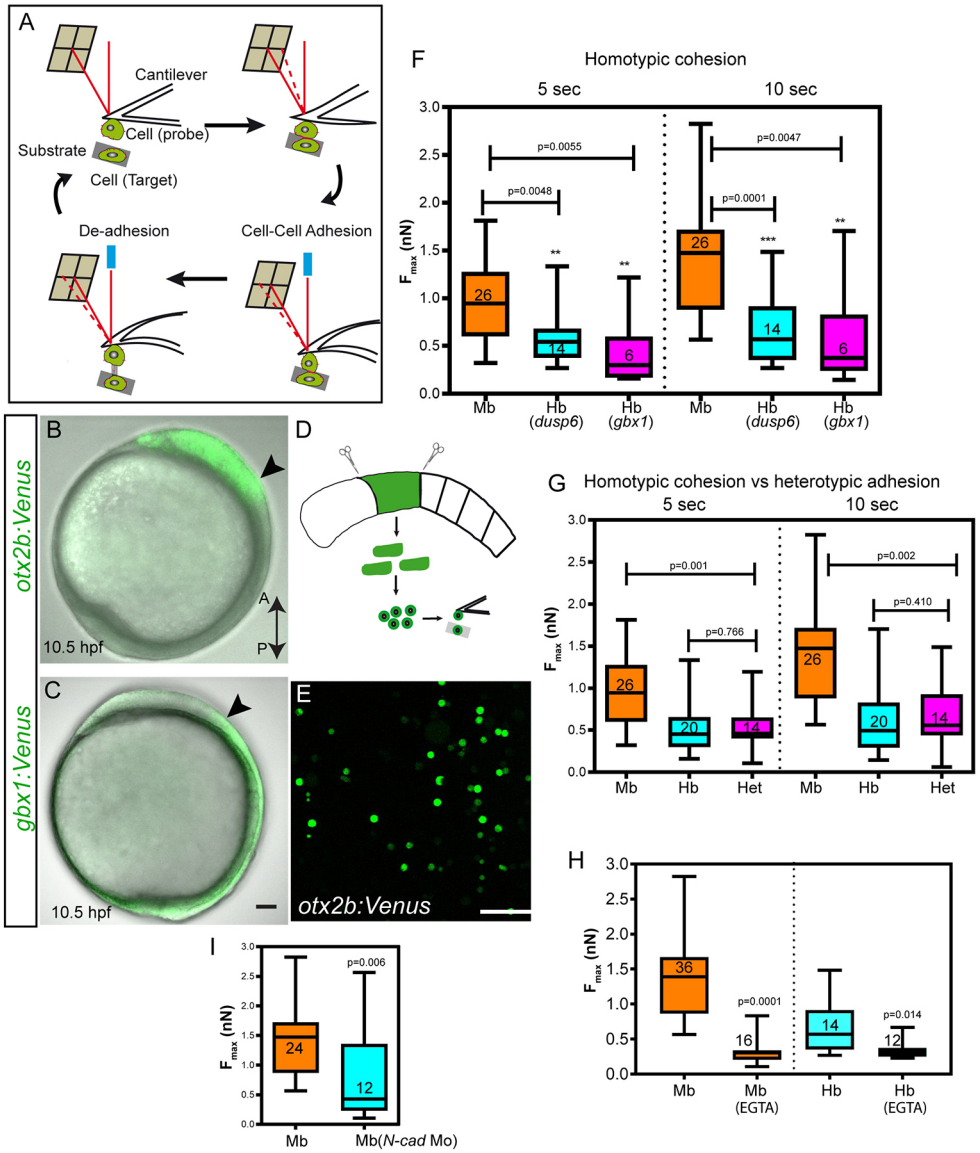

Fig. 5. Differential adhesion as a mechanism of cell sorting at the MHB. (A) Schematic representation of atomic force microscope-based single cell force spectroscopy (AFM-SCFS). A cell attached to the cantilever is brought into contact with another cell placed on the substrate (approach). During cell-cell contact, adhesion molecules form bonds in the contact zone. After a predefined contact time, the cantilever is retracted, which results in the breaking of bonds between the two cells (retract); thus, the maximum force (Fmax, measured in nanonewtons, nN) required to separate the two cells can be measured (redrawn based loosely on Krieg et al., 2008). (B,C) Lateral views *of otx2b:Venus* (midbrain, Mb) and *gbx1:Venus* (hindbrain, hb) embryos at 10.5 hpf; arrowheads indicate the prospective MHB. (D,E) The embryos were dissociated at the tail bud stage and a single-cell suspension for SCFS was made by mechanical trituration. (F,G) Midbrain cells (*otx2b*:Venus-positive) showed more cohesion than hindbrain cells (*gbx1* or *dusp6* positive) at the 5 s and 10 s time points (homotypic adhesion), while heterotypic adhesion between Mb with Hb cells was lower than that of Mb-Mb cohesion. The *P* values (comparison between Mb and Hb; Mann–Whitney *U*-test) for the two time points are shown on the graph; *n* represents the number of cell pairs analyzed for each condition. (H) Depletion of Ca^{2+} using 5 mM EGTA addition dramatically reduced cell-cell cohesion between Mb and Hb cells. (I) Depletion of N-cadherin using a morpholino-mediated knockdown (N-cad Mo) reduced cell-cell cohesion between *otx2b*-positive cells (midbrain cells); *n* represents the number of cell pairs analyzed and is indicated within the box and whisker plot. All AFM-based experiments were repeated at least three times. Data are shown using box and whisker plots: the ends of the box are the upper and lower quartiles and the box spans the interquartile range; median is marked within the box; whiskers indicate maximum and minimum values.

embryos at the one-cell stage, the number of such *fgf8a*-derived cells in the midbrain was higher compared with control fish (Fig. 6G,H). These results indicate that Eph-ephrin signaling is involved in cell sorting at the MHB.

Recently, actomyosin and Yap-mediated mechanisms have also been shown to be essential for maintaining rhombomere boundaries in zebrafish (Calzolari et al., 2014; Voltes et al., 2019). However, our analysis with F-actin reporters and active Yap signaling reporter did not reveal any involvement during MHB formation (Fig. S3), probably because both actomyosin-mediated tension and Yap appear much later at the hindbrain boundaries (Cayuso et al., 2019; Voltes et al., 2019). Therefore, these results suggest that, at the MHB, N-cad mediates cell-cell adhesion and that Eph/ephrin signaling is involved in cell sorting, both of which serve to establish and maintain sharp gene expression boundaries at the MHB.

DISCUSSION

Using multiple transgenic reporter fish for lineage tracing and live imaging, we show that lineage restriction and the formation of sharp gene expression boundaries in the developing MHB occur through

Development (2020) 147, dev186882. doi:10.1242/dev.186882

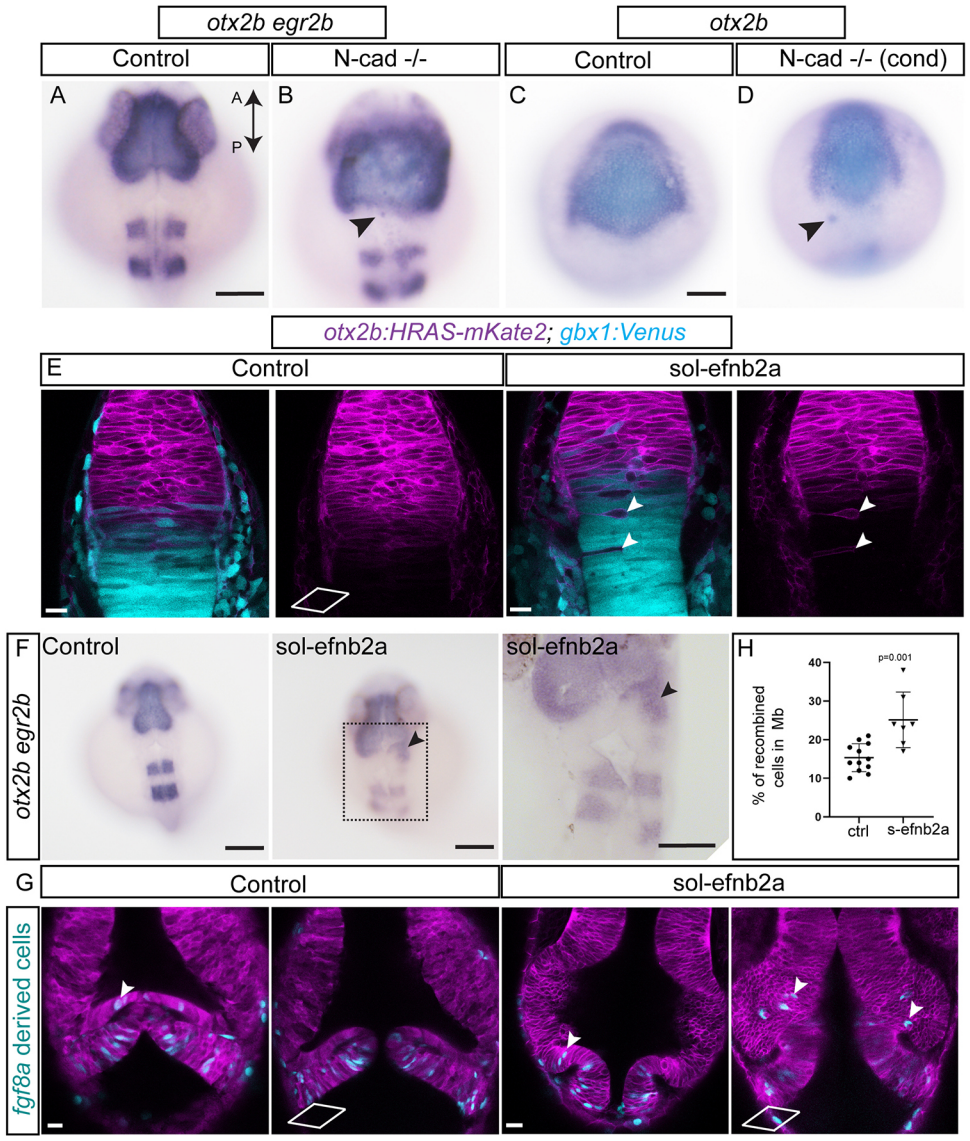

Fig. 6. Molecular mechanisms of cell sorting at the MHB. To test whether N-cadherin (*cdh2*) plays a role in cell sorting, two approaches using CRISPR/Cas9-mediated mutant analysis were used. First, exons 1 and 2 of N-cadherin were targeted to generate global N-cad$^{-/-}$ embryos by injecting the sgRNA with Cas9 mRNA at the one-cell stage. (A,B) *In situ* hybridization analysis of mutant embryos at 24 hpf for *otx2b* and *egr2b* showed a disorganized pattern with fuzzy gene expression boundaries for both markers compared with control embryos. Individual *otx2b* cells outside their expression domain are also seen (arrowheads). This phenotype was observed in 35% of the embryos analyzed (*n*=26). Second, using Cre/lox-controlled Cas9 combined with the *otx2b:CreER*^{T2} driver, N-cad was conditionally (cond) ablated in the *otx2b* domain. (C,D) Conditional perturbation of N-cad in the midbrain resulted in irregular gene expression boundaries (*otx2b*) and a few cells outside the expression domain (arrowheads). This phenotype was observed in 42% of the embryos analyzed (*n*=90). Soluble efnb2a (sol-efnb2a) was injected as mRNA in one-cell stage embryos in the *otx2b:HRAS-mKate2*; *gbx1:venus* double transgenic line. (E) Perturbed Eph-ephrin signaling resulted in mis-sorting of cells across the MHB, presence of single *otx2b*-positive cells in the hindbrain (arrowheads) and *otx2b*-positive, *gbx1*-positive cells distributed further away from the Otx-Gbx overlapping domain. (F) *In situ* hybridization analysis of embryos analyzed at 24 hpf for *otx2b* and *egr2b* showed the presence of *otx2b*-positive cells outside their expression domain in sol-efnb2a-injected embryos (arrowheads; region marked with a dotted rectangle is enlarged in the panel below). This phenotype was observed in 44% of the embryos analyzed (*n*=206). (G) Embryos of the *Tg(fgf8a:CreER*^{T2}*)*; *Tg(hsp70l:loxP-DsRed-loxP-EGFPNLS)* cross were injected with sol-efnb2a and HRAS-mKate2 (to mark cell membrane) at the one-cell stage. 4-OH tamoxifen-mediated recombination was induced at 6 hpf. Embryos were heat shocked at 24 hpf (to label recombined cells) and imaged at 36 hpf. Perturbed Eph-ephrin signaling resulted in greater numbers of *fgf8*-derived cells in the midbrain domain (arrowheads). Two representative sections from the dorsal (top) and ventral (bottom) domains are shown. (H) Quantification of *fgf8a*-derived recombined cells in the midbrain (control versus s-efnb2a) showed greater cell numbers in s-efnb2a-treated embryos. A two-tailed, unpaired *t*-test was used to calculate statistical significance; each point in the graph represents an individual embryo with the mean and s.e.m. shown (control, ctrl, *n*=12; s-efb2a, *n*=7; *P*=0.0010). Scale bars: 100 µm in A-D,F; 20 µm in E,G.

multiple complementary mechanisms, namely cell-fate plasticity and cell sorting, and that these processes involve differential adhesion, N-cad and Eph-ephrin signaling (Fig. 7).

Previously, in zebrafish, using RNA *in situ* hybridization, we found that, at 60% epiboly (6 hpf), the anterior border of the *gbx1* expression domain directly abuts the *otx2b* domain, with an overlap of the two domains covering three or four cell layers; this structure subsequently resolves into sharply defined non-overlapping adjacent segments (Rhinn et al., 2003). Owing to technical limitations (fixed samples) and the absence of reporter lines,

Development (2020) 147, dev186882. doi:10.1242/dev.186882

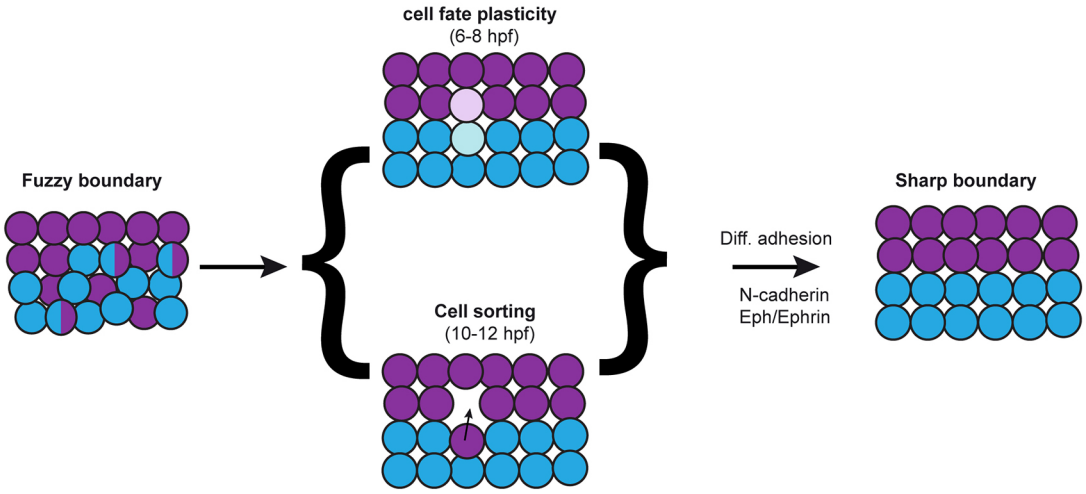

Fig. 7. Multiple mechanisms help establish sharp midbrain-hindbrain boundary. Schematic representation of how a fuzzy boundary develops into a sharp boundary over time, which involves complementary mechanisms such as cell-fate plasticity and cell sorting, with the latter entailing differential adhesion, N-cadherin and Eph-ephrin signaling.

these overlapping and segregation events could not be visualized by live imaging or be lineage traced to follow their fate in these earlier studies. Here, using various knock-in fluorescent reporters and Cre driver lines to visualize and follow cell fate, we show that cell-fate plasticity does occur across the gene expression domains abutting the developing MHB. This phenomenon predominantly occurs during early gastrulation stages (6-8 hpf) and reduces by the end of gastrulation (10 hpf). A possible explanation for this phenomenon is as follows. Morphogens such as Wnt (in the midbrain domain) and Fgf (in the hindbrain domain), transcription factors such as engrailed 1, engrailed 2, Pax2, Pax5 and Pax8 (across the MHB), and cell-adhesion molecules, including Eph/ephrin (present in adjacent domains), are expressed only between 8 and 10 hpf. Thus, the presence of such a multitude of factors can increase cellular complexity and lead to reinforced fate commitment and lineage restriction.

Comparable results from other studies support this explanation. For example, a recent study on zebrafish hindbrain development demonstrated cell identity switching through a mechanism involving segment identity and retinoic acid signaling, with intermingling between segments and consequent cell-identity changes occurring during early stages of rhombomere segment formation, i.e. before the establishment of robust Eph/ephrin signaling that causes cell segregation across rhombomere boundaries (Addison et al., 2018). Likewise, using a combination of cell transplantation, iontophoretic cell labeling and live-cell imaging, we found that lineage restriction occurs at the MHB during the late gastrulation stages in zebrafish (Langenberg and Brand, 2005; Langenberg et al., 2006), with similar observations being reported in chick and mice (Zervas et al., 2004; Sunmonu et al., 2011; Tossell et al., 2011). Similarly, cell lineage analysis during hindbrain development in chick has shown that the clonal progeny of cells labeled before the establishment of morphological boundaries display plasticity in cell-fate specification; in contrast, clones labeled after boundary formation are confined to their respective segments (Fraser et al., 1990).

Interestingly, we have noted a consistent pattern in our lineage-tracing results, i.e. whereas *gbx1*-postive cells in the midbrain domain are always also *otx2b* positive (double positive) and are relatively fewer in number, *otx2b*-positive cells in the hindbrain domain are rarely *gbx1* positive and are relatively greater in number. Although there are a few potential explanations, currently, there are no known molecular mechanisms that can adequately explain this observation.

Between 10 and 12 hpf, when the neural plate transforms into the neural keel, convergent extension occurs, involving extensive cell intercalation, cell division and intermingling of cells along the A-P axis (Kimmel et al., 1994), suggesting that mechanisms other than cell-fate switching may exist to maintain sharp expression boundaries. Consistently, using live imaging, we show that cells actively sort at the MHB between 10 and 12 hpf, and that this sorting is influenced by N-cad-mediated adhesion between the midbrain and hindbrain cells. These findings are consistent with previous data on the role of N-cad in cell convergence and maintenance of neuronal positioning during vertebrate neural tube development (Lele et al., 2002).

Over the years, three major classes of cell segregation mechanisms during boundary formation have been uncovered. The first is based on differential cell-cell adhesive property (differential adhesion hypothesis) that establishes interfacial tension across boundaries (Steinberg, 2007). The second is actomyosin-based establishment of cortical tension (differential tension hypothesis) at the boundaries (Harris, 1976), and the third involves cell-cell repulsion mediated by Eph/ephrin-like signaling molecules. These mechanisms, either individually or in combination, have been shown to establish and maintain boundaries in different tissues during development (Batlle and Wilkinson, 2012). Furthermore, in the developing spinal cord of zebrafish, it has been recently shown that a heterogeneous population of neuronal progenitors induced by sonic hedgehog signaling sort to rearrange and form sharply bordered domains, and that this sorting mechanism is mediated via N-cadherin (Xiong et al., 2013). Here, using an AFM-based assay to measure cell-adhesion properties, we show that the prospective midbrain and hindbrain cells indeed have differential adhesive strengths and that adhesion between a midbrain and a hindbrain cell is lower than that of a midbrain-midbrain cell combination. Time lapse movies of MHB formation show extensive cell movement and intermingling during which cells constantly change their partners. Intuitively, such cell behavior would require differential adhesion because this

Development (2020) 147, dev186882. doi:10.1242/dev.186882

intermingling and subsequent sorting leads to compartmentalization of similar cells that ultimately form a pattern.

Additionally, our data also reveal that the cell-adhesion molecule N-cadherin is involved in contributing to this adhesion. Thus, in a scenario where adhesion is disrupted due to N-cad mutations, it is expected that cells will mis-sort, and we show that conditional N-cad mutants indeed display sorting defects at the MHB. These observations highlight the importance of differential adhesion during boundary formation at the MHB.

Interactions between Eph receptor tyrosine kinase and its ligand ephrin are known to control multiple cell biological processes such as polymerization of actin cytoskeleton, cadherin function and integrin-mediated adhesion (Batlle and Wilkinson, 2012). Several Eph receptors and their ligands are expressed in complementary domains in multiple tissues during development (e.g. in the developing rhombomere boundaries), and any perturbation in the signaling leads to cell intermingling between adjacent segments (Xu et al., 1999). However, loss-of-function studies using Eph/ephrin mutants are complicated due to redundancy among the many receptors and ligands expressed in the same tissue/cell type *in vivo* (Bush and Soriano, 2012). Nonetheless, using a soluble version of the ligand Efnb2a to block a wide range of Eph/ephrin bidirectional signaling, we find that Eph/ephrin signaling plays a significant role in establishing sharp gene expression boundaries. Further studies are required to identify the specific molecular combination of Eph receptors and ligands that mediate cell sorting at the MHB. Notably, individual perturbations of N-cad and Eph/ephrin signaling did not yield a comprehensive sorting phenotype in any of the embryos (i.e. it is never 100%), suggesting that both differential adhesion and Eph/ephrin pathway are required for sharpening the boundary at the MHB. Interestingly, previous studies and subsequent concept reviews have posited that Eph-ephrin signaling may drive cell segregation through heterotypic tension/repulsion by interplay with Ca^{2+}-dependent cell-adhesion molecules like cadherins (Rohani et al., 2014; Winklbauer, 2015), and that differential expression of N-cad may not be necessary as changes in activity mediated by Eph/ephrin signaling or heterotypic tension alone are sufficient to facilitate cell segregation (Canty et al., 2017; Taylor et al., 2017). Thus, further investigations into the mechanical aspects of how Eph/ephrin signaling can modulate cadherin function and repulsion/tension at the cell-cell interface will provide greater clarity on this extremely complex process.

In summary, using novel fluorescent knock-in reporters, live imaging, Cre driver-based lineage tracing, and cutting-edge cell adhesion assays and mutant analysis, we describe the process of lineage restriction at the MHB. It occurs through multiple complementary mechanisms, which are, in sequence, cell-fate specification, lineage restriction and cell sorting; the last involving differential adhesion, N-cad and Eph-ephrin signaling.

MATERIALS AND METHODS

Zebrafish maintenance and breeding

Zebrafish (*Danio rerio*) embryos and adults were obtained, maintained and raised as described previously (Brand et al., 2002; Westerfield, 2000). Embryos were staged as hours post fertilization (hpf) (Kimmel et al., 1995). The wild-type strain AB was used to obtain knock-in lines, and transgenic fish lines were maintained as outcrosses. None of the larvae or adult fish showed any physiological or behavioral abnormalities.

All animal experiments were carried out in accordance with animal welfare laws of the Federal Republic of Germany (Tierschutzgesetz) that were enforced and approved by the competent local authority (Landesdirektion Sachsen; protocol numbers TVV21/2018; DD24-5131/346/11 and DD24-5131/346/12; TVT1/2019), by the institutional animal welfare committee (Tierschutzkommission der Technische Universität Dresden) and in accordance with EU directives (Directive 2010/63/EU).

CRISPR/Cas9-mediated knock-in lines

The knock-in lines for various genes expressed at MHB were generated and maintained as previously described (Kesavan et al., 2017, 2018). The target site sequence and primers for generating baits are provided in Table S1. Transgenic animals used in this study are listed in Table S2.

DNA, RNA and morpholino microinjections in zebrafish embryos

mRNA for *HRAS:mKate2* or *soluble-efnb2a* were prepared using mMessage mMachine Kit (ThermoFisher). 100 pg of mRNA in a 1 nl volume was microinjected into one-cell stage embryos (wildtype AB). For N-cadherin morpholino experiments, 0.5 pmol/embryo was injected in a 1 nl volume (wildtype AB). Plasmids and morpholinos used in this study are listed in Table S3.

Global and conditional N-cadherin mutants

For generating a global N-cadherin mutant, a 1 nl of solution containing 25 ng/µl of the two sgRNAs (Target sequence in Table S1) and 150 ng/µl of Cas9 mRNA was injected into one-cell stage embryos (wildtype AB). PCR genotyping of embryos absolutely correlated with the mutant phenotype and the two sgRNA showed high efficiency in cutting the target site.

For generating the N-cadherin conditional mutants, 1 nl of solution containing 25 ng/µl of the two sgRNAs and 25 ng/µl of circular plasmid DNA (*Hsp70l:loxp_nonFP_loxp_Cas9eGFP*) were injected into one-cell stage embryos obtained from *otx2:CreET*^{T2}. 4-OH tamoxifen (5 µM) induction was carried out at 4 hpf and embryos were heat shocked at 8 hpf for 30 min at 37°C. Embryos were sorted for eGFP fluorescence at 10.5 hpf and fixed for further analysis using *in situ* hybridization.

In situ hybridization

Embryos at specific developmental stages were derived by crossing wild-type fish (Ab strain). They were fixed in 4% PFA, stored in 100% methanol at −20°C and whole-mount *in situ* hybridization was performed as described elsewhere (Kesavan et al., 2017; Reifers et al., 1998). Briefly, using a RNA labeling and detection kit (Roche), digoxigenin (DIG)-labeled probes were synthesized from linear DNA and the hybridized probes were detected using anti-digoxigenin antibody. Antibody staining was visualized using BM purple (digoxigenin). *In situ* probe staining for *otx2*, *gbx1* and *gbx2* (Rhinn et al., 2003), and *wnt1* (Lekven et al., 2003) matched expression patterns described previously.

Live imaging

For live imaging, early somite stage embryos (10 to 12 hpf) were embedded in 0.7% low melting agarose. Late somite stage embryos (15 hpf onwards) were treated with 1-phenyl-2-thiourea (PTU) to block pigmentation, and with MS-222 for anesthesia then were mounted on a glass-bottomed dish (MatTek) in 1% low melting agarose. All embryos were imaged on a Zeiss LSM 780. Images were analyzed using FIJI (open source software) or Imaris (v7, Bitplane), respective TIFF files were generated and figures assembled in Adobe Photoshop (version CS5 or CS6). For time-lapse imaging, tissue sections spanning 30-40 µm, with a *z* interval of 1 µm, were imaged every 2 min and 30 s at 28°C on the LSM780 (Zeiss) microscope. The duration of time-lapse imaging was different for each imaging experiment and is mentioned in the legend of the respective figures. Maximum intensity projections of fluorescence and transmitted light images were generated using Imaris (v7, Bitplane), FIJI (Schindelin et al., 2012) or Arivis 4D. Cell tracking was carried out using FIJI (Trackmate).

4-OH-tamoxifen-mediated recombination

The Cre drivers *otx2b:CreER* ^{T2} and *fgf8a:CreER* ^{T2} fish were crossed with the zebrabow responder line *Tg(ubb:lox2272-loxp-RFP-lox2272-CFP-loxp-YFP)* (Pan et al., 2013) or with *Tg(hsp70l:loxP-DsRed-loxP-EGFPNLS)* (Knopf et al., 2011). Embryos were treated with 1 µM 4-OH-tamoxifen (4-OHT) at 6 hpf for 12 h or with 10 µM 4-OH-tamoxifen at 24 hpf for 12 h. Control embryos were left untreated. All embryos were live imaged at 48 hpf

as described above. In the zebrabow responder, a cell with multiple copies of RFP, CFP and YFP, CreER^{T2}-mediated stochastic recombination events lead to cell clones being labeled by different colors. The combinatorial nature of fluorescent protein expression gives a unique barcode to each cell and marks their progenies with the same color. Untreated embryos show only default RFP expression, i.e. they represent non-recombined cells.

Atomic force microscopy-based single cell force spectroscopy (AFM-SCFS)

The AFM-SCFS was performed as previously described (Krieg et al., 2008). AFM-SCFS is a high-precision force measuring tool that measures the difference in adhesion strength between two cells by initially bringing two isolated cells into contact. Next, after a given contact time, the cells are separated and the force required to separate them is quantified. All experiments and data analyses used the Nanowizard I AFM setup (JPK Instruments). Briefly, cantilevers (Nano world TR-TL-Au-20, nominal spring constant k=32 mN m^{-1}) that were coated with concanavalin A (ConA, 2.5 mg/µl, Sigma) were used. Two regions were marked in a glass-bottomed dish; one was coated with bovine serum albumin (1%) to obtain a non-adhesive substrate, while the other was coated with ConA (2.5 mg/µl) to obtain an adhesive substrate. Both substrates were gently rinsed with the 1×HBSS (Life Technologies) before the experiment.

Transgenic embryos staged between 10 and 10.5 hpf were carefully dissected to isolate midbrain or hindbrain progenitors, and a single-cell suspension was obtained by trituration that was diluted in 1×HBSS and seeded onto the substrate. For both homotypic and heterotypic adhesion experiments, cells were identified using fluorescence microscopy, whereas for heterotypic adhesion experiments, fluorescent dextran, labeled with Cy5, was injected into only one set of embryos to distinguish between the two cell types. A given 'probe'-cell was selected from the non-adhesive side of the substrate with a ConA-coated cantilever by gently pressing on it with a controlled force of 1 nN, typically for 1 s. The cell was removed from the surface for 2-10 min to allow it to firmly attach to the cantilever. The probe cell was then moved above a 'target' cell that was firmly attached to the adhesive (ConA-coated) part of the substrate. Adhesion experiments ('force-distance cycles', see Fig. 1A) were performed at contact force of 1 nN, 10 µm s^{-1} approach and retract velocities, and contact times of either 5 or 10 s. Each condition (i.e. same probe-target couple at the same contact time) was repeated up to three times, with a resting time of 30 s between successive contacts. Each probe cell was used to test several target cells and no more than 12 curves were obtained with any given probe cell. Cells were observed continuously during and between the force-distance cycles to judge whether they were intact and were firmly attached to the cantilever or substrate. Force-distance curves were derived and pooled data were used for statistical analysis (Graph pad prism, v8). Cadherin dependence of cell adhesion was tested after either depleting calcium by adding EGTA (5 mM, Sigma) to the medium, or by injecting embryos with morpholino oligonucleotides for N-cadherin (2 ng, Genetools).

Statistical analysis

Data are presented as mean±s.e.m., unless specified otherwise. A two-tailed, unpaired t-test was used to calculate statistical significance at P<0.05 (GraphPad prism, v8.0).

Acknowledgements

We are thankful to the Chen and Wente labs for providing plasmids to generate Cas9 and sgRNA mRNA (via Addgene); to Jens Ehrig (Molecular Imaging and Manipulation Facility, CMCB, Dresden), Jens Friedrichs, the Heisenberg lab and the Guck lab for help with various AFM experiments; to past and present members of the Brand lab for discussions; to Pablo Sanchez Quintana for help with imaging; and to Dr Vasuprada Iyengar for language and content editing. We thank Marika Fischer, Jitka Michling and Daniela Mögel for dedicated zebrafish care. The Light Microscopy Facility at CMCB also supported this work.

Competing interests

The authors declare that the research was conducted in the absence of any commercial or financial relationships that could be construed as a potential conflict of interest.

Author contributions

Conceptualization: G.K., M.B.; Methodology: G.K., A.M., S.H.; Validation: G.K.; Formal analysis: G.K.; Resources: G.K., A.M., S.H.; Writing - original draft: G.K., M.B.; Writing - review & editing: G.K., S.H., M.B.; Visualization: G.K.; Supervision: M.B.; Project administration: M.B.; Funding acquisition: M.B.

Funding

This work was supported by project grants from the Deutsche Forschungsgemeinschaft (BR 1746/6-1, BR 1746/6-2 and BR 1746/3) and by a European Research Council advanced grant (Zf-BrainReg) to M.B. G.K. was supported by post-doctoral fellowships from the Vetenskapsrådet and by a European Molecular Biology Organization long-term fellowship (ALTF 350-2011).

Supplementary information

Supplementary information available online at
http://dev.biologists.org/lookup/doi/10.1242/dev.186882.supplemental

Peer review history

The peer review history is available online at
https://dev.biologists.org/lookup/doi/10.1242/dev.186882.reviewer-comments.pdf

References

Addison, M., Xu, Q., Cayuso, J. and Wilkinson, D. G. (2018). Cell identity switching regulated by retinoic acid signaling maintains homogeneous segments in the hindbrain. *Dev. Cell* **45**, 606-620.e3. doi:10.1016/j.devcel.2018.04.003

Arias, A. M. and Steventon, B. (2018). On the nature and function of organizers. *Development* **145**, dev159525. doi:10.1242/dev.159525

Astone, M., Lai, J. K. H., Dupont, S., Stainier, D. Y. R., Argenton, F. and Vettori, A. (2018). Zebrafish mutants and TEAD reporters reveal essential functions for Yap and Taz in posterior cardinal vein development. *Sci. Rep.* **8**, 1-15. doi:10.1038/s41598-018-27657-x

Batlle, E. and Wilkinson, D. G. (2012). Molecular mechanisms of cell segregation and boundary formation in development and tumorigenesis. *Cold Spring Harb. Perspect Biol.* **4**, a008227. doi:10.1101/cshperspect.a008227

Behrndt, M., Salbreux, G., Campinho, P., Hauschild, R., Oswald, F., Roensch, J., Grill, S. W. and Heisenberg, C.-P. (2012). Forces driving epithelial spreading in zebrafish gastrulation. *Science* **338**, 257-260. doi:10.1126/science.1224143

Brand, M., Granato, M. and Nüsslein-Volhard, C. (2002). Keeping and raising zebrafish. In *Zebrafish: A Practical Approach* (ed. C. Nüsslein-Volhard and R. Dahm), pp. 7-37. Oxford: Oxford University Press.

Bush, J. O. and Soriano, P., (2012). Eph/ephrin signaling: genetic, phosphoproteomic, and transcriptomic approaches. *Semin. Cell Dev. Biol.* **23**, 26-34. doi:10.1016/j.semcdb.2011.10.018

Calzolari, S., Terriente, J. and Pujades, C. (2014). Cell segregation in the vertebrate hindbrain relies on actomyosin cables located at the interhombomeric boundaries. *EMBO J.* **33**, 686-701. doi:10.1002/embj.201386003

Canty, L., Zarour, E., Kashkooli, L., François, P. and Fagotto, F. (2017). Sorting at embryonic boundaries requires high heterotypic interfacial tension. *Nat. Commun.* **8**, 1-15. doi:10.1038/s41467-017-00146-x

Cavodeassi, F., Ivanovitch, K. and Wilson, S. W. (2013). Eph/Ephrin signalling maintains eye field segregation from adjacent neural plate territories during forebrain morphogenesis. *Development* **140**, 4193-4202. doi:10.1242/dev.097048

Cayuso, J., Xu, Q., Addison, M. and Wilkinson, D. G. (2019). Actomyosin regulation by Eph receptor signaling couples boundary cell formation to border sharpness. *ELife* **8**, e49696. doi:10.7554/eLife.49696

Cooke, J., Moens, C., Roth, L., Durbin, L., Shiomi, K., Brennan, C., Kimmel, C., Wilson, S. and Holder, N. (2001). Eph signalling functions downstream of Val to regulate cell sorting and boundary formation in the caudal hindbrain. *Development* **128**, 571-580.

Cooke, J. E., Xu, Q., Wilson, S. W. and Holder, N. (1997). Characterisation of five novel zebrafish Eph-related receptor tyrosine kinases suggests roles in patterning the neural plate. *Dev Gene Evol* **206**, 515-531. doi:10.1007/s004270050082

Cooke, J. E., Kemp, H. A. and Moens, C. B. (2005). EphA4 is required for cell adhesion and rhombomere-boundary formation in the zebrafish. *Curr. Biol.* **15**, 536-542 doi:10.1016/j.cub.2005.02.019

Dahmann, C., Oates, A. C. and Brand, M. (2011). Boundary formation and maintenance in tissue development. *Nat. Rev. Genet.* **12**, 43-55. doi:10.1038/nrg2902

Dworkin, S. and Jane, S. M. (2013). Novel mechanisms that pattern and shape the midbrain-hindbrain boundary. *Cell. Mol. Life Sci.* **70**, 3365-3374. doi:10.1007/s00018-012-1240-x

Fraser, S., Keynes, R. and Lumsden, A. (1990). Segmentation in the chick embryo hindbrain is defined by cell lineage restrictions. *Nature* **344**, 431-435. doi:10.1038/344431a0

Gibbs, H. C., Chang-Gonzalez, A., Hwang, W., Yeh, A. T. and Lekven, A. C. (2017). Midbrain-Hindbrain Boundary Morphogenesis: At the Intersection of Wnt and Fgf Signaling. *Front. Neuroanat.* **11**. doi:10.3389/fnana.2017.00064

Harris, A. K. (1976). Is cell sorting caused by differences in the work of intercellular adhesion? A critique of the steinberg hypothesis. *J. Theor. Biol.* **61**, 267-285. doi:10.1016/0022-5193(76)90019-9

Jiang, Y. J., Brand, M., Heisenberg, C. P., Beuchle, D., Furutani-Seiki, M., Kelsh, R. N., Warga, R. M., Granato, M., Haffter, P., Hammerschmidt, M. et al. (1996). Mutations affecting neurogenesis and brain morphology in the zebrafish, Danio rerio. *Development* **123**, 205-216.

Kesavan, G., Chekuru, A., Machate, A. and Brand, M. (2017). CRISPR/Cas9 mediated zebrafish knock-in as a novel strategy to study midbrain-hindbrain boundary development. *Frontiers in Neuroanatomy* **11**, 52. doi:10.3389/fnana.2017.00052

Kesavan, G., Hammer, J., Hans, S. and Brand, M. (2018). Targeted knock-in of CreER^{T2} in zebrafish using CRISPR/Cas9. *Cell Tissue Res.* **372**, 41-50. doi:10.1007/s00441-018-2798-x

Kiecker, C. and Lumsden, A. (2005). Compartments and their boundaries in vertebrate brain development. *Nat. Rev. Neurosci.* **6**, 553-564. doi:10.1038/nrn1702

Kimmel, C. B., Warga, R. M. and Kane, D. A. (1994). Cell cycles and clonal strings during formation of the zebrafish central nervous system. *Development* **120**, 265-276.

Kimmel, C. B., Ballard, W. W., Kimmel, S. R., Ullmann, B. and Schilling, T. F. (1995). Stages of embryonic development of the zebrafish. *Dev. Dyn.* **203**, 253-310. doi:10.1002/aja.1002030302

Knopf, F., Hammond, C., Chekuru, A., Kurth, T., Hans, S., Weber, C. W., Mahatma, G., Fisher, S., Brand, M. and Schulte-Merker, S. (2011). Bone regenerates via dedifferentiation of osteoblasts in the zebrafish fin. *Dev. Cell* **20**, 713-724. doi:10.1016/j.devcel.2011.04.014

Krieg, M., Arboleda-Estudillo, Y., Puech, P. H., Kafer, J., Graner, F., Muller, D. J. and Heisenberg, C. P. (2008). Tensile forces govern germ-layer organization in zebrafish. *Nat. Cell Biol.* **10**, 429-436. doi:10.1038/ncb1705

Langenberg, T. and Brand, M. (2005). Lineage restriction maintains a stable organizer cell population at the zebrafish midbrain-hindbrain boundary. *Development* **132**, 3209-3216. doi:10.1242/dev.01862

Langenberg, T., Dracz, T., Oates, A. C., Heisenberg, C. P. and Brand, M. (2006). Analysis and visualization of cell movement in the developing zebrafish brain. *Dev. Dyn.* **235**, 928-933. doi:10.1002/dvdy.20692

Lekven, A. C., Buckles, G. R., Kostakis, N. and Moon, R. T. (2003). Wnt1 and wnt10b function redundantly at the zebrafish midbrain–hindbrain boundary. *Dev. Biol.* **254**, 172-187. doi:10.1016/S0012-1606(02)00044-1

Lele, Z., Folchert, A., Concha, M., Rauch, G.-J., Geisler, R., Rosa, F., Wilson, S. W., Hammerschmidt, M. and Bally-Cuif, L. (2002). parachute/n-cadherin is required for morphogenesis and maintained integrity of the zebrafish neural tube. *Development* **129**, 3281-3294.

Li, X., Zhao, X., Fang, Y., Jiang, X., Duong, T., Fan, C., Huang, C.-C. and Kain, S. R. (1998). Generation of destabilized green fluorescent protein as a transcription reporter. *J. Biol. Chem.* **273**, 34970-34975. doi:10.1074/jbc.273.52.34970

Molina, G. A., Watkins, S. C. and Tsang, M. (2007). Generation of FGF reporter transgenic zebrafish and their utility in chemical screens. *BMC Dev. Biol.* **7**, 62. doi:10.1186/1471-213X-7-62

Pan, Y. A., Freundlich, T., Weissman, T. A., Schoppik, D., Wang, X. C., Zimmerman, S., Ciruna, B., Sanes, J. R., Lichtman, J. W. and Schier, A. F. (2013). Zebrabow: multispectral cell labeling for cell tracing and lineage analysis in zebrafish. *Development* **140**, 2835-2846. doi:10.1242/dev.094631

Raible, F. and Brand, M. (2004). Divide et Impera–the midbrain-hindbrain boundary and its organizer. *Trends Neurosci.* **27**, 727-734. doi:10.1016/j.tins.2004.10.003

Reifers, F., Bohli, H., Walsh, E. C., Crossley, P. H., Stainier, D. Y. and Brand, M. (1998). Fgf8 is mutated in zebrafish acerebellar (ace) mutants and is required for maintenance of midbrain-hindbrain boundary development and somitogenesis. *Development* **125**, 2381-2395.

Rhinn, M. and Brand, M. (2001). The midbrain–hindbrain boundary organizer. *Curr. Opin. Neurobiol.* **11**, 34-42. doi:10.1016/S0959-4388(00)00171-9

Rhinn, M., Lun, K., Amores, A., Yan, Y. L., Postlethwait, J. H. and Brand, M. (2003). Cloning, expression and relationship of zebrafish gbx1 and gbx2 genes to Fgf signaling. *Mech. Dev.* **120**, 919-936. doi:10.1016/S0925-4773(03)00135-7

Rhinn, M., Picker, A. and Brand, M. (2006). Global and local mechanisms of forebrain and midbrain patterning. *Curr. Opin. Neurobiol.* **16**, 5-12. doi:10.1016/j.conb.2006.01.005

Rohani, N., Parmeggiani, A., Winklbauer, R. and Fagotto, F. (2014). Variable combinations of specific ephrin Ligand/Eph receptor pairs control embryonic tissue separation. *PLoS Biol.* **12**, e1001955. doi:10.1371/journal.pbio.1001955

Schindelin, J., Arganda-Carreras, I., Frise, E., Kaynig, V., Longair, M., Pietzsch, T., Preibisch, S., Rueden, C., Saalfeld, S., Schmid, B. et al. (2012). Fiji: an open-source platform for biological-image analysis. *Nat. Methods* **9**, 676-682. doi:10.1038/nmeth.2019

Snapp, E. L. (2009). Fluorescent proteins: a cell biologist's user guide. *Trends Cell Biol.* **19**, 649-655. doi:10.1016/j.tcb.2009.08.002

Steinberg, M. S. (2007). Differential adhesion in morphogenesis: a modern view. *Curr. Opin. Genet. Dev.* **17**, 281-286. doi:10.1016/j.gde.2007.05.002

Sunmonu, N. A., Li, K., Guo, Q. and Li, J. Y. (2011). Gbx2 and Fgf8 are sequentially required for formation of the midbrain-hindbrain compartment boundary. *Development* **138**, 725-734 doi:10.1242/dev.055665

Taylor, H. B., Khuong, A., Wu, Z., Xu, Q., Morley, R., Gregory, L., Poliakov, A., Taylor, W. R. and Wilkinson, D. G. (2017). Cell segregation and border sharpening by Eph receptor–ephrin-mediated heterotypic repulsion. *J. R. Soc. Interface* **14**, 20170338. doi:10.1098/rsif.2017.0338

Tossell, K., Kiecker, C., Wizenmann, A., Lang, E. and Irving, C. (2011). Notch signalling stabilises boundary formation at the midbrain-hindbrain organiser. *Development* **138**, 3745-3757. doi:10.1242/dev.070318

Träber, N., Uhlmann, K., Girardo, S., Kesavan, G., Wagner, K., Friedrichs, J., Goswami, R., Bai, K., Brand, M., Werner, C. et al. (2019). Polyacrylamide bead sensors for in vivo quantification of cell-scale stress in zebrafish development. *Sci. Rep.* **9**, 1-14. doi:10.1038/s41598-019-53425-6

Voltes, A., Hevia, C. F., Engel-Pizcueta, C., Dingare, C., Calzolari, S., Terriente, J., Norden, C., Lecaudey, V. and Pujades, C. (2019). Yap/Taz-TEAD activity links mechanical cues to progenitor cell behavior during zebrafish hindbrain segmentation. *Development* **146**. doi:10.1242/dev.176735

Weber, I. P., Ramos, A. P., Strzyz, P. J., Leung, L. C., Young, S. and Norden, C. (2014). Mitotic Position and Morphology of Committed Precursor Cells in the Zebrafish Retina Adapt to Architectural Changes upon Tissue Maturation. *Cell Reports* **7**, 386-397. doi:10.1016/j.celrep.2014.03.014

Westerfield, M. (2000). *The Zebrafish Book. A Guide for the Laboratory Use of Zebrafish (Danio rerio)*, 4th edn. Eugene: University of Oregon Press.

Winklbauer, R. (2015). Cell adhesion strength from cortical tension - an integration of concepts. *J. Cell. Sci.* **128**, 3687-3693. doi:10.1242/jcs.174623

Wurst, W. and Bally-Cuif, L. (2001). Neural plate patterning: upstream and downstream of the isthmic organizer. *Nat. Rev. Neurosci.* **2**, 99-108. doi:10.1038/35053516

Xiong, F., Tentner, A. R., Huang, P., Gelas, A., Mosaliganti, K. R., Souhait, L., Rannou, N., Swinburne, I. A., Obholzer, N. D., Cowgill, P. D. et al. (2013). Specified neural progenitors sort to form sharp domains after noisy Shh signaling. *Cell* **153**, 550-561. doi:10.1016/j.cell.2013.03.023

Xu, Q., Mellitzer, G., Robinson, V. and Wilkinson, D. G. (1999). In vivo cell sorting in complementary segmental domains mediated by Eph receptors and ephrins. *Nature* **399**, 267-271. doi:10.1038/20452

Zervas, M., Millet, S., Ahn, S. and Joyner, A. L. (2004). Cell behaviors and genetic lineages of the mesencephalon and rhombomere 1. *Neuron* **43**, 345-357. doi:10.1016/j.neuron.2004.07.010